Sea surface height observations of the 34ºN ‘waveguide’ in the North Atlantic

David Cromwell

James Rennell Division for Ocean Circulation and Climate,

Southampton Oceanography Centre, Southampton SO14 3ZH, U.K.

Revised version: May, 2001

Geophysical Research Letters

Corresponding author address: David Cromwell, James Rennell Division for Ocean Circulation and Climate, Southampton Oceanography Centre, European Way, Southampton SO14 3ZH, U.K. E-mail: ddc@soc.soton.ac.uk

ABSTRACT

We present a study of the energetic zonal band at 34ºN in the North Atlantic using a wavelet analysis of more than 8 years of TOPEX/POSEIDON altimeter data. It is already well-established in the literature that this zonal ‘waveguide’ is dominated by large-scale propagating features. The wavelet analysis yields sea surface height variance at a range of periods and wavelengths, allowing us to observe and quantify evolution of the features in space and time. Signal variance west of the mid-Atlantic ridge at 34ºN is larger than to the east of the ridge: by a factor of ~2 in the period band 0.5-0.9 years, in which baroclinic Rossby waves and eddies propagate. The period of the peak energy is reduced crossing the ridge from ~1 year to ~7-9 months, before rising again to the annual cycle on the other side. There is also evidence of energy peaks at periods of ~2-4 years in the Gulf Stream region and east of the ridge.

1. INTRODUCTION

Several recent studies have revealed particularly interesting ocean dynamics in a zonal strip around 34^{o}N in the northeast Atlantic, in the vicinity of the subtropical front/Azores Current. These features are thought to be baroclinic Rossby waves [*Cipollini et al., 1997*], [*Cipollini et al., 1999*] or periodic eddies known as STORMs (SubTropical Oceanic Rings of Magnitude) [*Pingree and Sinha, 1998*]. A recent theoretical study examining the role of bathymetry on baroclinic Rossby wave propagation yields a concentration of propagating energy in a zonal band at, or near, near this latitude [*Killworth and Blundell, 1999*]. The objective of the present paper is not to settle the question of whether propagating signals in the 34^{o}N waveguide are Rossby waves or STORMs (or both), but to quantify the variance in sea surface height (SSH); in particular, variations in space and time.

Time series analysis of SSH anomalies have typically been based upon Fourier analysis or related methods such as the Radon transform [*Deans, 1983*]. However, interpretation of such analysis assumes stationarity in the dataset under investigation, an assumption which is almost certainly not valid. Indeed, propagating features are likely to change their characteristics as they traverse an ocean basin, varying with depth of thermocline, bathymetry, local density profile, and so on. In order to detect and quantify such changes within a data series, we require a technique that can analyse local variations within a data series. The wavelet transform is such a method. In section 2, we discuss the processing and analysis of TOPEX/POSEIDON SSH data, including the use of wavelet analysis (in both space and time) in determining local power spectra. Section 3 presents the results of the wavelet analysis of the altimeter data and, in section 4, we draw conclusions and make some suggestions for future work.

2. DATA PROCESSING AND ANALYSIS

2.1 TOPEX/POSEIDON Data

The TOPEX/POSEIDON (hereafter T/P) satellite, launched in August 1992, lays down a ground track of passes 2.7^o apart in longitude, repeated every 9.92 days. We applied a standard set of corrections for orbit errors, atmospheric delays, tides and sea state effects to collocated data (see [*Cipollini et al., 1997*]).

Sea surface height (SSH) anomalies are computed over the global ocean relative to the mean SSH calculated from the data for 1993-1995. (This 3-year mean was chosen to reduce any bias resulting from active El Niño years). The accuracy of the SSH retrieval with T/P is of the order of 2 cm [*Cheney et al., 1994*]. Each cycle of data is then interpolated onto a 1º by 1º grid. The interpolation, which uses a Gaussian weighted mean of all the data within 200 km of a grid point, reduces the instrument and correction errors whilst leaving the larger scale signal relatively unaffected. In this study we use 306 T/P cycles, spanning October 1992 – January 2001.

2.2 Wavelet analysis

The wavelet method allows one to analyse localised power variations within a discrete series at various scales [*Foufoula-Georgiou and Kumar, 1994*]. Wavelets can be considered as building blocks in a decomposition or series expansion, using dilated and translated versions of a mother wavelet, each multiplied by an appropriate coefficient [*Farge, 1992*]. The local wavelet power spectrum is the square of the wavelet coefficients [*Torrence and Compo, 1998*]. The global wavelet spectrum is the average spectrum over all time, equivalent to the Fourier spectrum. We make the usual choice here of adopting the Morlet wavelet, which is a complex-valued, modulated Gaussian plane wave, widely used in the study of geophysical processes. It is given by $\psi(\eta) = \pi^{-1/4} e^{i\omega\eta} e^{-\eta^2/2}$, where ω is the nondimensional frequency which must be equal to, or greater than, 5 to satisfy the wavelet admissibility condition [*Farge, 1992*].

3. ANALYSIS

3.1 Wavelet spectra at point locations in the '34ºN waveguide'

In this paper, we restrict attention to the previously reported zonal band of high-energy propagating features near 34ºN in the northeast Atlantic which, for convenience, we here term the '34ºN waveguide'. We apply a wavelet analysis in this waveguide for the first time, as far as we are aware, to try to detect and quantify changes in variance, frequency and wavenumber content of the SSH signals. We examine T/P time series data at grid points separated by 1º in longitude along the zonal waveguide at 34ºN. At each location we calculate from the time series data: the local wavelet spectrum, the global wavelet spectrum and a scale-averaged time series (in order to home in on specific periodic features of interest). We also perform a wavelet analysis in space, along the longitude dimension, to examine possible chnages in wavenumber content. From previous studies in this region (e.g. [*Cipollini et al., 1997*] and [*Pingree and Sinha, 1998*]), it is known that propagating features, whether eddies or baroclinic Rossby waves, occur at periodicities of ~6-10 months. We therefore perform scale-averaging in the period band 0.5-0.9 years. Examples are given in Figure 1 for the locations 43^{o}W and 28^{o}W in the 34^{o}N waveguide. The dashed contours in Figures 1b and 1f indicate the cone of influence, below which edge effects may be important [*Torrence and Compo, 1998*]. Note from Figures 1b and 1f that the frequency content changes with time: something which a conventional Fourier analysis would not detect. The solid contour in Figures 1b and 1f indicates the 98% confidence level, assuming a white-noise background spectrum defined by the variance and number of points of the original time series. Dashed contours in Figures 1c,d,g and h indicate the 98% confidence level. At 28^{o}W the strongest peak occurs at, or close to, the annual period, corresponding to the seasonal steric effect (Fig 1g). Secondary peaks occur at ~7 months, corresponding to known propagating Rossby waves and/or eddies, and a tertiary peak at ~20 months. There is also a peak at ~4 years, though this must be treated with caution because of the limited length of the time series. The time series of the scale-average wave power in the period range 0.5-0.9 years (Fig 1h) have maxima around February 1993, April 1995, August 1997 and August 2000. Further west, at 43^{o}W, the strongest peak now occurs close to 8 months, again consistent with known properties of propagating Rossby waves and/or eddies, with the second strongest peak at the annual cycle (Fig 1c). There is a tertiary peak around 18 months, and longer-period peaks that, once again, are probably not well-defined due to the finite length of the time series. In the 0.5-0.9 year scale-average band, there are peaks in June 1996 and September 1998 (Fig 1d). Examining time series of scale-average wave power at many successive locations, similar to Figures 1d and 1h, shows westward propagation of features. Objective estimation of speed in a particular period band can be done using the Radon transform (e.g. [*Chelton and Schlax, 1996*], [*Polito and Cornillon, 1997*] and [*Cipollini et al., 1999*]) applied to the real part of the wavelet transform for that period band. This is analogous to bandpass filtering with the passband corresponding to the period band of interest (G. Compo, pers. comm., 2001). In the eastern basin (between 38^o-8^{o}W) the estimated speed is ~2.9 cm/s; in the western basin (75^o-39^{o}W), the speed is higher at ~4.1 cm/s, consistent with the deeper thermocline there. These speeds tally with previously reported findings (e.g. [*Chelton and Schlax, 1996*] and [*Cipollini et al., 1997*]).

3.2 Peaks in the global wavelet spectra

Let us now examine the global wavelet spectra at 34^{o}N, as plotted in Figure 2a, with the corresponding bathymetric section from [*Smith and Sandwell, 1997*] shown in Figure 2b. Note that each vertical (constant-longitude) slice in Figure 2a corresponds to a global wavelet spectrum at a particular location, as plotted in Figures 1c,f. The solid contour indicates the 98% confidence level. At 34^{o}N, the strength of variance in signals west of the mid-Atlantic ridge is larger than to the east of the ridge: approximately twice as large in the period band 0.5-0.9 years, corresponding to first-mode baroclinic Rossby waves and/or eddies. In particular, wavelet power rises on the west-facing downward slope of the ridge (~38^o-48^{o}W).

The dominant period, i.e. the period of the peak energy, is reduced crossing the ridge, from the annual cycle to a period of ~7-9 months, before rising again to the annual period. There is also evidence of longer-period energy at periods 2-4 years between ~65^o - 75^{o}W (Gulf Stream region) and east of the ridge (25^o - 35^{o}W). Applying wavelet analysis in space (along the longitude axis) at different times (T/P cycles), yields power spectra as a function of wavelength (Figure 2c). This confirms the location where variance changes abruptly: between ~38^o-48^{o}W, on the west-facing downward slope of the ridge. Peak energy occurs at wavelengths in a band of ~500-1000 km. This is consistent with reported observations that the dominant propagating features at 34^{o}N have wavelengths of ~500 km ([*Cipollini et al., 1997*] and [*Pingree and Sinha, 1998*]).

3.3 Power Hovmöller plots (longitude-time diagrams)

If we scale-average the wavelet power spectra of sea surface height anomaly data at a number of locations, we can examine the temporal *and* spatial variability of the SSH features. Figure 3a shows such a 'power Hovmöller' plot [*Torrence and Compo, 1998*] for 34^{o}N in the period band from 0.5-0.9 years, corresponding to the propagating features of interest. Figure 3b is the zonal average of the data field in Figure 3a. The time-averaged field is shown in Figure 3c. Note that wavelet power west of the ridge (~0.005 m^2) is more than twice that on the east of the ridge (~0.002 m^2), with peak values on the west-facing downward slope of the ridge (0.007 m^2). The maximum power in this period range occurs in October 1995, perhaps because of enhanced atmospheric forcing or baroclinic instability of the Azores Current around this time. However, a thorough analysis is outside the scope of this paper. Edge effects reduce the wavelet power over a few months at the start and end of the time series.

Note that it is *not* appropriate to use wavelet power Hovmöller plots to estimate propagation speeds of single travelling waves. This can be understood by considering the idealised case of a perfect sine wave at each longitude (similar to a narrow bandpass plot). In this case, and neglecting edge effects, the wavelet power will just be a constant with time, regardless of longitude. No propagation would therefore be observed in the power Hovmöller plot. On the other hand, packets of waves moving with a particular group velocity *would* appear as diagonal alignments in a power Hovmöller plot. Since it is not always clear whether one is observing quasi-continuous single Rossby wave events, or groups of Rossby waves, one should avoid inferring propagation speeds from power Hovmöller plots. Indeed, applying the Radon transform to the data in Figure 3a, in the expectation of estimating propagation speeds, yields speeds that are significantly too low: speeds of ~ 0.9 cm/s in the eastern basin and ~1.3 cm/s in the western basin. In short, wavelet power Hovmöller plots are useful for analysing changes in power with space or in time (applying the usual caution at the start/end of the time series) but do not tell us how fast travelling waves are moving (C. Torrence, pers. comm., 2001).

4. SUMMARY AND CONCLUDING REMARKS

We have investigated a zonal 'waveguide' of enhanced sea surface height variance at 34^{o}N in the north Atlantic using a wavelet analysis of more than 8 years of TOPEX/POSEIDON altimeter data. Use of the wavelet method allows analysis of the temporal and frequency characterisation of non-stationary signals. It is not generally understood why there should be a band of enhanced energy at this latitude, through baroclinic instability of the Azores Current [*Alves and Colin de Verdière, 1998*] and the effect of bathymetry (e.g. [*Killworth and Blundell, 1999*] and [*Tailleux and McWilliams, 2000*]) may both play a role.

The strength of variance in signals west of the mid-Atlantic ridge at 34^{o}N is greater than to the east of the ridge: approximately twice as great in the period band 0.5-0.9 years, corresponding to first-mode baroclinic Rossby waves and/or eddies. A change in Rossby wave amplitude crossing the ridge has been reported by [*Polito and Cornillon, 1997*], who suggest that a conversion of some energy from baroclinic to barotropic mode may be responsible. The period of peak energy is reduced crossing the ridge, from the annual cycle to a period of ~7-9 months, before rising again to the annual period. There is evidence of energy peaks at periods of ~2-4 years in the Gulf Stream region the (65^o-75^{o}W) and east of the ridge (35^o -45^{o}W). However, variance at periods greater than ~3 years falls below the cone of influence, and should probably be disregarded. Large-scale feature propagation (Rossby waves or eddies) occurs in the period range 0.5-0.9 years at speeds of ~ 2.9 cm/s in the eastern basin and ~4.1 cm/s in the western basin, consistent with previous estimates at this latitude. We intend to extend the scope of this work to a wavelet analysis of the global ocean using not just SSH data, but sea surface temperature and ocean colour data.

ACKNOWLEDGEMENTS

NASA and CNES provided the TOPEX/POSEIDON data, and Helen Snaith and Paolo Cipollini assisted in the processing. Useful comments were received from Jeff Blundell, Peter Challenor, Paolo Cipollini, Peter Killworth, Graham Quartly and Ian Robinson. Wavelet software, and advice on its use, was provided by Christopher Torrence and Gilbert Compo, and is available at URL: http://paos.colorado.edu/research/wavelets

REFERENCES

Alves, M. L. G. R. and A. Colin de Verdière, 1998: Instability dynamics of a subtropical jet and applications to the Azores Front current system: eddy-driven mean flow, *Journal of Physical Oceanography 29* (5), 837-864.

Chelton, D. B. and M. G. Schlax, 1996: Global observations of oceanic Rossby waves, *Science 272*, 234-238.

Cheney, R. E., L. Miller, R. Agreen, N. Doyle and J. Lillibridge, 1994: TOPEX/Poseidon: the 2-cm solution, *Journal of Geophysical Research 99*, 24,555-24,563.

Cipollini, P., D. Cromwell, M. S. Jones, G. D. Quartly and P. G. Challenor, 1997: Concurrent altimeter and infrared observations of Rossby wave propagation near 34°N in the Northeast Atlantic, *Geophysical Research Letters 24* (8), 889-892.

Cipollini, P., D. Cromwell and G. D. Quartly, 1999: Observations of Rossby wave propagation in the northeast Atlantic with TOPEX/POSEIDON altimetry, *Advances in Space Research 22* (11), 1553-1556.

Deans, S. R. (1983). The Radon Transform and some of its applications, John Wiley, New York.

Farge, M., 1992: Wavelet transforms and their applications to turbulence, *Annual review of Fluid Mechanics 24*, 395-457.

Foufoula-Georgiou, E. and P. Kumar (1994). Wavelets in Geophysics, Academic Press, San Diego.

Killworth, P. D. and J. R. Blundell, 1999: The effect of bottom topography on the speed of observed and theoretical long extra-tropical planetary waves, *Journal of Physical Oceanography 29*, 2689-2710.

Pingree, R. D. and B. Sinha, 1998: Dynamic Topography (ERS-1/2 and seatruth) of subtropical ring (STORM 0) in the STORM corridor (32-34°N, Eastern Basin, North Atlantic Ocean, *Journal of the Marine Biological Association of the UK 78*, 351-376.

Polito, P. S. and P. Cornillon, 1997: Long baroclinic Rossby waves detected by TOPEX/POSEIDON, *Journal of Geophysical Research 102* (C2), 3215-3235.

Smith, W. H. F. and D. T. Sandwell, 1997: Global Seafloor Topography from Satellite Altimetry and Ship Depth Soundings, *Science 277* (26 September, 1997), 1956-1962.

Tailleux, R. and J. C. McWilliams, 2000: Acceleration, creation, and depletion of wind-driven, baroclinic Rossby waves over an ocean ridge, *Journal of Physical Oceanography 30*, 2186-2213.

Torrence, C. and G. P. Compo, 1998: A practical guide to wavelet analysis, *Bulletin of the American Meteorological Society 79* (1), 61-78.

FIGURE CAPTIONS

Figure 1. Wavelet analysis of TOPEX/POSEIDON sea surface height anomaly data in the northeast Atlantic at two sample locations: 34°N, 43°W (a-d) and 34°N, 28°W (e-h). (a) time series of height anomaly data. (b) wavelet power spectrum. Dashed line indicates the cone of influence, below which edge effects become important, and the solid contour is the 98% confidence level. (c) the global wavelet power spectrum; dashed contour is the 98% confidence level. (d) the scale-average time series for the period-band 0.5 – 0.9 years; (e)-(h): as for (a)-(d), respectively.

Figure 2. (a) Global wavelet spectrum in the zonal waveguide at 34°N. The solid contour is the 98% confidence level. Note the dominant period drops from 1 year to ~7-9 months between ~48°-40°W. (b) bathymetric section at 34°N. The mid-Atlantic ridge is between ~45°-25°W. (c) Local power spectrum as function of wavelength. Note the strong variance in the wavelength band 500-1000 km on the westward-facing downward slope of the ridge, cf. (a).

Figure 3. (a) A power Hovmöller plot at 34°N of 0.5-0.9-yr averaged wavelet power in sea surface height. The solid contour is the 98% confidence level; (b) the average of (a) over all longitudes; (c) the time-average of (a).

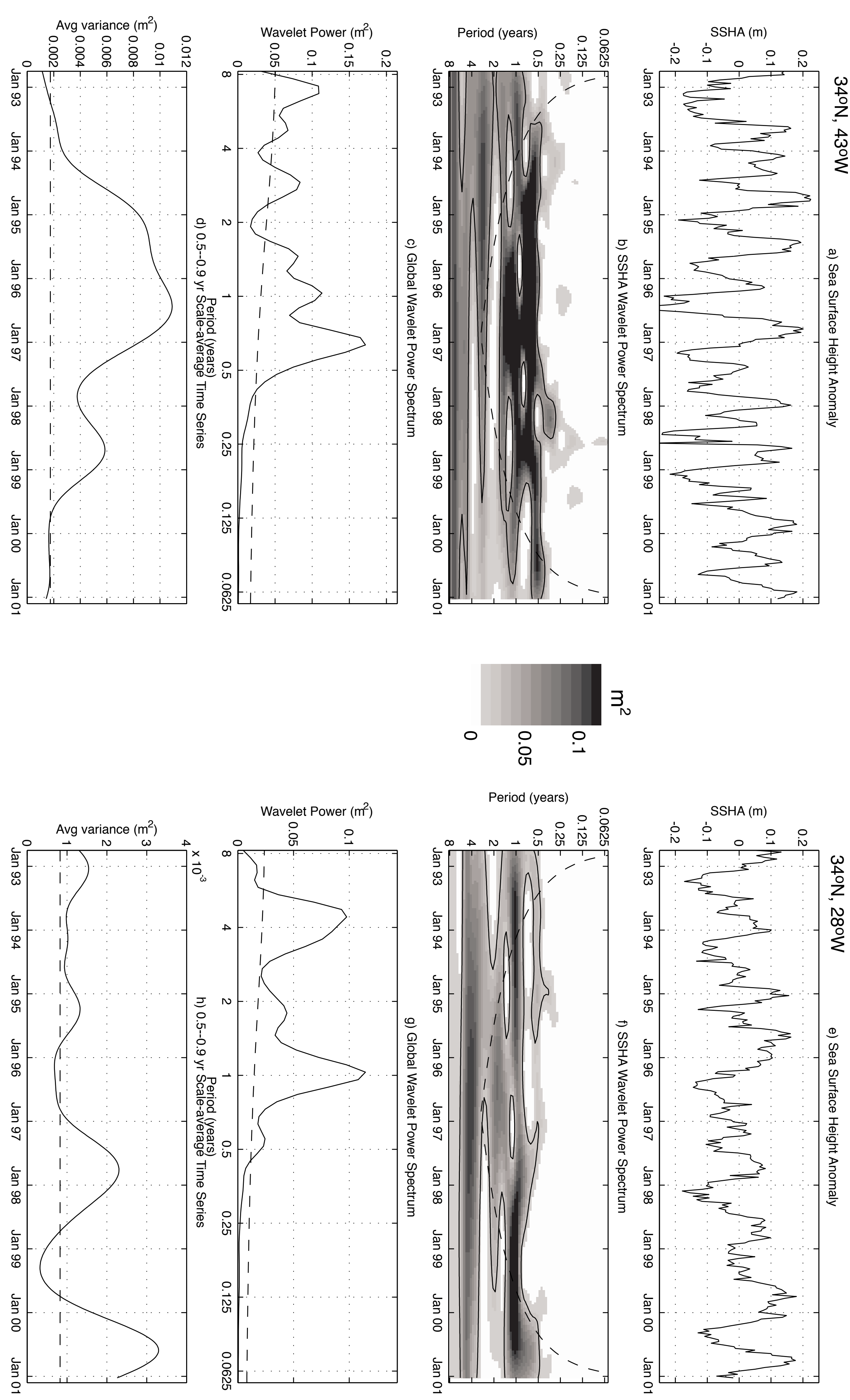

34°N, 43°W
a) Sea Surface Height Anomaly
SSHA (m)
b) SSHA Wavelet Power Spectrum
Period (years)
c) Global Wavelet Power Spectrum
Wavelet Power (m2)
d) 0.5--0.9 yr Scale-average Time Series
Avg variance (m2)
Period (years)
m2
34°N, 28°W
e) Sea Surface Height Anomaly
f) SSHA Wavelet Power Spectrum
g) Global Wavelet Power Spectrum
h) 0.5--0.9 yr Scale-average Time Series
x 10-3
Jan 93
Jan 94
Jan 95
Jan 96
Jan 97
Jan 98
Jan 99
Jan 00
Jan 01

Figure 1

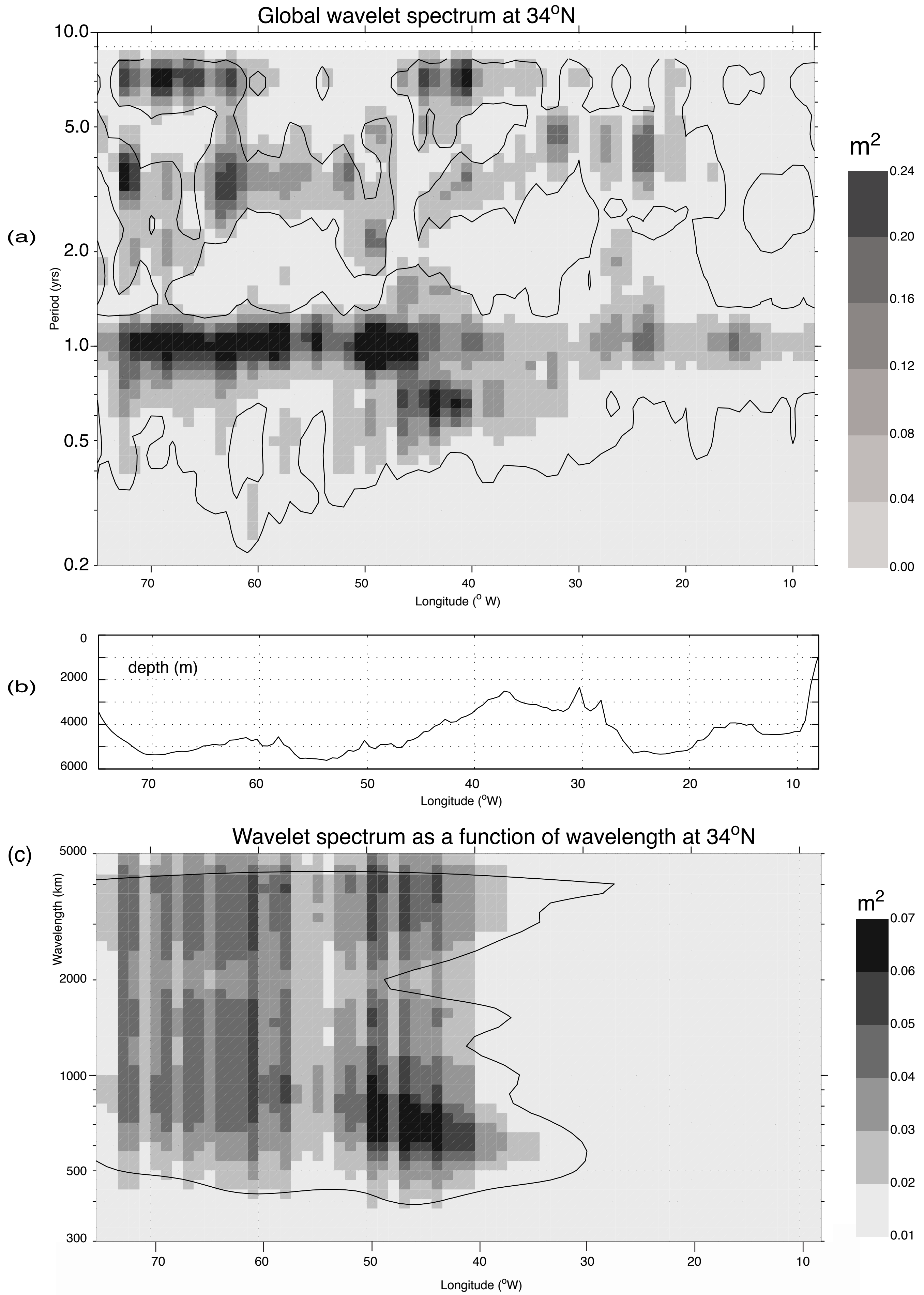

Global wavelet spectrum at 34°N
(a)
Period (yrs)
10.0
5.0
2.0
1.0
0.5
0.2
70
60
50
40
30
20
10
Longitude (° W)
m²
0.24
0.20
0.16
0.12
0.08
0.04
0.00
(b)
depth (m)
0
2000
4000
6000
Longitude (°W)
Wavelet spectrum as a function of wavelength at 34°N
(c)
Wavelength (km)
5000
2000
1000
500
300
m²
0.07
0.06
0.05
0.04
0.03
0.02
0.01

Figure 2

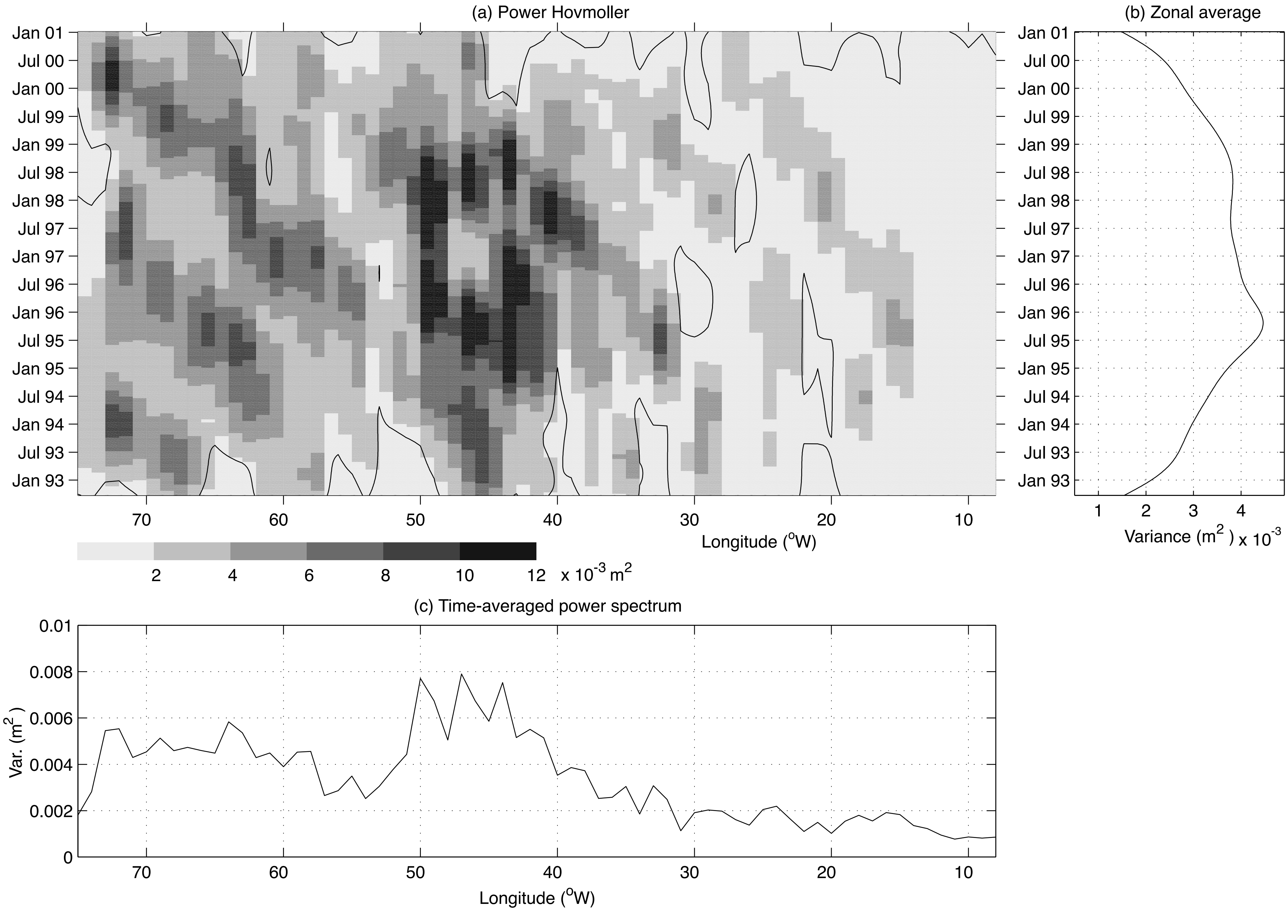

(a) Power Hovmoller
Jan 01
Jul 00
Jan 00
Jul 99
Jan 99
Jul 98
Jan 98
Jul 97
Jan 97
Jul 96
Jan 96
Jul 95
Jan 95
Jul 94
Jan 94
Jul 93
Jan 93
70
60
50
40
30
20
10
Longitude (°W)
2
4
6
8
10
12
x 10^-3 m^2
(b) Zonal average
1
2
3
4
Variance (m^2) x 10^-3
(c) Time-averaged power spectrum
0.01
0.008
0.006
0.004
0.002
0
Var. (m^2)
Longitude (°W)

Figure 3